Bulletin of Research Center for Computing and Multimedia Studies,
Hosei University, **27** (2013)
Published online (http://hdl.handle.net/10114/8198)

Development of the Transformer for Contactless Power Suppliers

Tatsuya OHASHI1), Iliana MARINOVA2) and Yoshifuru SAITO1)

[1)] *Graduate School of Hosei University, Tokyo 184-8584, Japan*
[2)] *Technical University of Sofia, Sofia 1756, Bulgaria*

SUMMARY

Contactless power supplier is composed of a transformer having the distinct primary and secondary coils separated by air gap. Because of the electromagnetic compatibility problem, it is essential to keep the leakage magnetic fields around the contactless power supplier as low as possible.
This paper carries out the wavelets multi-resolution analysis to the magnetic field distributions around contact-less power supplier. As a result, we have succeeded in obtaining one of the reasonable core shapes by observing the wavelets spectra of measured magnetic field vector distributions. Furthermore, it is revealed that a tested trial transformer gives nearly 80 percent power transmission efficiency even though the primary and secondary coils are separated by 10mm air gap.

KEY WORDS: contactless power suppliers, magnetic field visualization, discrete wavelets, multi-resolution analysis.

1. INTRODUCTION

Development of modern semiconductor technology makes it possible to realize small and light weight electronic devices equipped with a large variety of smart functions such as smart cellar phone as well as ultra mobile computers.

Although these electronics provide the highly efficient job environment, entertainments and convenient electronic consumer life, environments around human life are filling up with the electromagnetic fields. Particularly, because of the many electric power suppliers to supply the electronic products, it is essentially accompanied the electric power lines jangle, which leads to SAR (specific absorption rate) problems.

One of the solutions of this electromagnetic compatibility problem in the human life environment is to work out the cordless contactless power suppliers [1].

This paper concerns with development of a transformer composed of the separated primary and secondary cores by air gap. This transformer having the open magnetic flux paths between the primary and secondary core is of the paramount part to realize the contact-less power suppliers.

Apply the discrete wavelets transform to the magnetic field vector distributions around the transformer having open magnetic flux paths clarifies that the dish like ferrite cores embedding spirally wound coils gives a far excellent magnetic field vector distribution compared with those with conventional U shape cores [2,3]. An extension of conventional inner core type transformer employing U shape cores spreads the magnetic fields around the transformer centered at the air gaps. On the other side, a flat transformer employing dish shape ferrite cores and spirally wound coils (called the "flat transformer" in short) confines the magnetic fields at the center of the flat transformer, which minimizes the magnetic fields around the transformer.

As a first stage, we have worked out the trial flat transformers. Experimental study utilizing secondary resonant technique reveals that our flat transformer with 1cm air gap and 0.69 coupling factor is capable to transmit 79 percent input power to the secondary circuits [4]. Further, multi-resolution analysis of the discrete wavelets clarifies the effect of secondary resonance circuits, i.e., the highest level the magnetic field vector distributions visualizes the distinct difference of the magnetic field vector distributions between the secondary resonant and not resonant conditions.

Copyright © 2013 Hosei University

Received 9 March 2013
Published online 30 June 2013

2. Visualization of the Magnetic Field Around the Transformers

2.1 Transformer employing U shape ferrite core

Fig.1 shows the tested transformer employing two U shape ferrite cores. Table 1 lists specification of this transformer.

We have carried out the measurements of magnetic field vector distributions around this transformer using a search coil. The shape of this coil is a finite length solenoid and dimensions are the 1cm length, 14mm diameter, 30 turn wound coil using a 0.2mm diameter conducting wire. By means of this search coil, we have measured the magnetic field vector distributions.

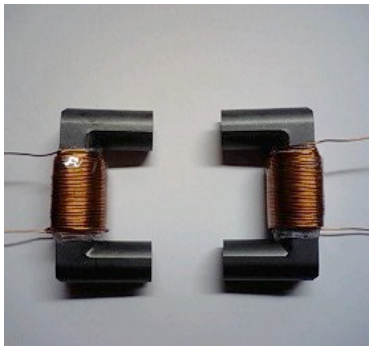

Fig.1 Tested transformer employing U shape ferrite cores.

Table 1 Specification of the transformer employing U shape cores.

U shape core	TDKPE22UU
Number of turns of primary coil	30turns
Number of turns of secondary coil	30turns
Diameter of primary coil	0.4mm
Diameter of secondary coil	0.4mm

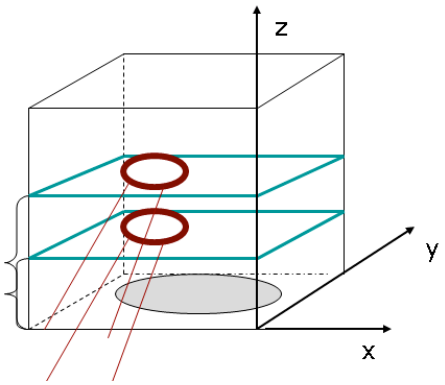

Fig.2 Scheme for measurement of the magnetic field vector distribution.

Fig. 2 shows a scheme for measurement of the magnetic field vector distribution. In this figure, the circular coils are the search coils. Two parallel surfaces illustrates the magnetic field measurement surfaces in the direction of z-axis component. Number of measured points is 8×8×4 with respect to the x-, y-, z-directions. Secondary circuit is no load and primary is excited by a 10kHz sinusoidal 0.5A current. The air gap between the heads of both primary and secondary U shape ferrite cores is of 1 cm.

Fig.3 shows one of the measured magnetic field vector distributions at some instance. It is obvious that the magnetic field vectors distribute around the U shape cores.

Copyright © 2013 Hosei University

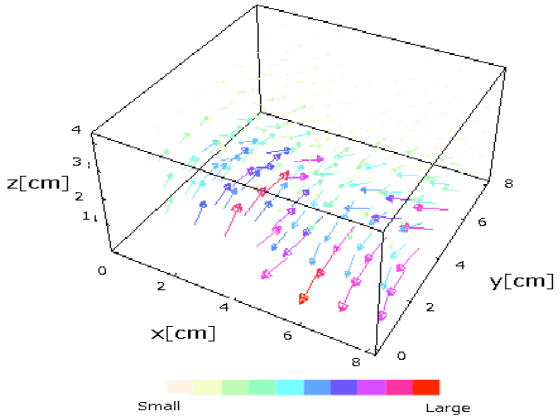

Fig.3 Magnetic field vector distribution around the transformer employing U shape ferrite cores.

2.2 Flat Transformer

The transformer employing U shape cores is essentially one of the extensions of in-core type transformer. On the other side, the flat transformer is one of the extensions of shell type transformer. Fig. 4 shows the tested flat transformer employing dish like ferrite cores. The dish like ferrite cores are composed of the Manganese and Zinc compound, and their customized products have been worked out by Tokin company.

Experimental measurement of the magnetic field vector distributions is carried out by means of the same search coil used to the transformer employing the U shape ferrite cores.

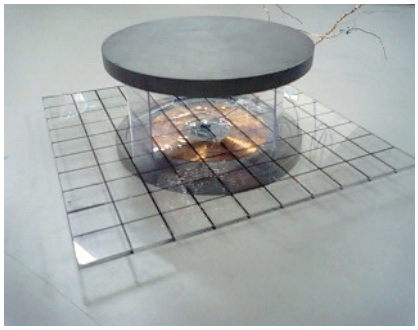

Fig. 4 Tested transformer employing the dish like ferrite cores.

Fig.5 shows a scheme of the magnetic field vector distribution measurements for this flat transformer. In this figure, the primary and secondary coils are spirally wound. Two parallel square surfaces illustrates the magnetic field measurement locations in the direction of z-axis component. Number of measured points is 8×8×4 with respect to the x-, y-, z-directions. The secondary circuit is no load and the primary circuit is excited by a 10kHz sinusoidal 0.5A current. The air gap between the primary and secondary core head surfaces is of 4 cm.

Table 2 lists specification of the flat shape transformer shown in Figs. 4 and 5.

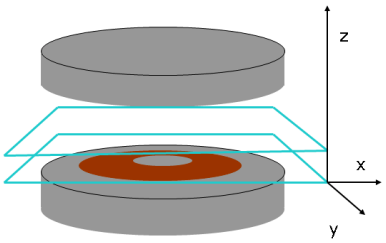

Fig.5 Scheme for measurement of the magnetic field vector distribution for the flat shape transformer.

Copyright © 2013 Hosei University

Table 2 Specification of the flat shape transformer.

Primary core: Outer diameter	105mm
Primary core: inner diameter	99mm
Primary core: thickness	7mm
Primary core: diameter	105mm
Primary core: depth of the cylinder cut	1mm
Primary core: length of the spiral winding	506.3mm
Primary core: diameter of the conductor	4mm
Secondary core: Outer diameter	105mm
Secondary core: inner diameter	99mm
Secondary core: thickness	7mm
Secondary core: diameter	105mm
Secondary core: depth of the cylinder cut	1mm
Secondary core: length of the spiral winding	506.3mm
Primary core: diameter of the conductor	4mm

Fig.6 shows one of the measured magnetic field vector distributions at some instance. It is obvious that the magnetic field vectors spreads over primary winding like a fountain, and also it is revealed that nature of the magnetic field distributions is intrinsically different between the in-core type in Fig.3 and shell- core type in Fig.6.

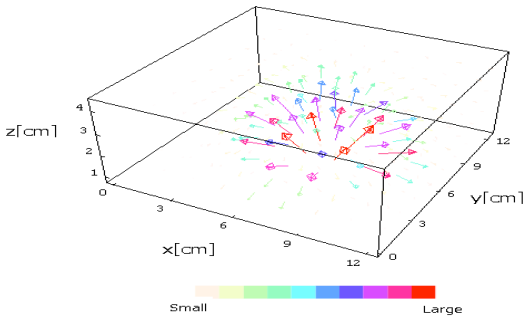

Fig.6 Magnetic field vector distribution between the flat shape cores.

3. The Wavelets Transform Analysis

3.1 Vector Wavelets Transform

The magnetic field vector distributions are generally three dimensional vectors. Therefore, when we apply the wavelets multi-resolution analysis to the three dimensional vectors, it leads to the three-dimensional vector wavelets transform [2,3].

When we denote a transpose operation of a three-dimensional (cubic) matrix Almn as

$$\left[A_{lmn}\right]^T = A_{mnl} \quad , \tag{1}$$

the three-dimensional wavelets spectrum matrix Slmn is given by

$$S_{lmn} = \left[W_n \cdot \left[W_m \cdot \left[W_l \cdot A_{lmn}\right]^T\right]^T\right]^T . \tag{2}$$

where the matrix Smn is a three-dimensional wavelets spectrum matrix with order l by m by n; and Wn, Wm and Wl are the wavelets transform matrix with order n by n, m by m and l by l, respectively.

The measured magnetic field vectors distribute in three-dimensionally so that the magnetic field vector distribution matrix Hlmn is composed of the three independent x-, y-, and z-vector component matrices X lmn, Y lmn, Z lmn, respectively.

The matrix Hlmn is represented by

$$\mathbf{H}_{lmn} = \mathbf{X}_{lmn} + \mathbf{Y}_{lmn} + \mathbf{Z}_{lmn} . \tag{3}$$

Copyright © 2013 Hosei University

Thus, the three-dimensional wavelets spectra of the magnetic field distribution are obtained by

$$\mathbf{S}_{lmn} = \left[W_n \cdot \left[W_m \cdot \left[W_l \cdot \left(\mathbf{X}_{lmn} + \mathbf{Y}_{lmn} + \mathbf{Z}_{lmn} \right) \right]^T \right]^T \right]^T \cdot \qquad (4).$$

Generally, the wavelets spectrum Slmn is classified into the multi-level spectra according to the orthogonal property of discrete wavelets transform. Number of levels p depends on not only the number of data comprising spectrum Slmn but also the wavelets base functions used for wavelets transform matrices Wn, Wm. Wl.

Apply the inverse wavelets transform to each of the decomposed wavelets spectra yields the wavelets multi-resolution result

$$\begin{aligned} \mathbf{H}_{lmn} &= \sum_{i=1}^{p} \mathbf{H}_{lmn}^{(p)} \\ &= \sum_{i=1}^{p} \left[W_n^T \cdot \left[W_m^T \cdot \left[W_l^T \cdot \mathbf{S}_{lmn}^{(i)} \right]^T \right]^T \right]^T, \end{aligned} \qquad (5)$$

where the levels 1,2, .. . p-th magnetic field vector distributions are $\mathbf{H}_{lmn}^{(1)}, \mathbf{H}_{lmn}^{(2)}, \cdots, \mathbf{H}_{lmn}^{(p)}$, respectively. Low and higher level magnetic field vector distributions represent the global and precise vector distributions, respectively. Sum of the entire levels gives the original vector field distribution.

3.2 Wavelets analysis of the magnetic field vector distribution around the transformer employing U shape ferrite cores

Fig.7 shows the wavelets spectra of the magnetic field vector distribution shown in Fig.3, where Daubechies second order base function is employed. It must be noted that wavelets transform to the vector fields gives the vector fields even in the wavelets spectrum space. Further, the most dominant wavelets spectrum vectors are extracted as observed in Fig. 7.

Because of the number of data in z-axis and also employed Daubechies second order base function, it is possible to obtain the three levels multi-resolution magnetic field vector distributions. These magnetic field vector distributions are shown in Fig. 8.

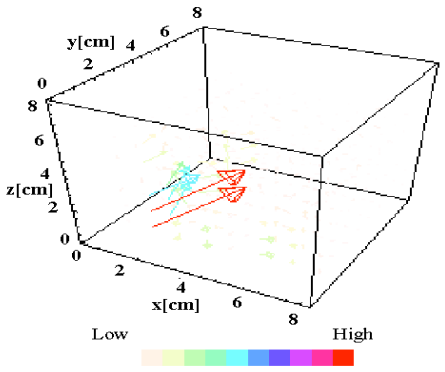

Fig.7 Wavelets spectra of the magnetic field vector distribution measured around the transformer employing U shape cores.

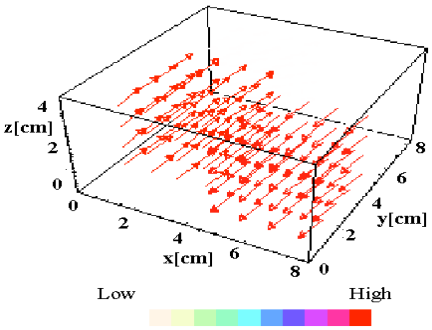

(a) Level p=1

Copyright © 2013 Hosei University

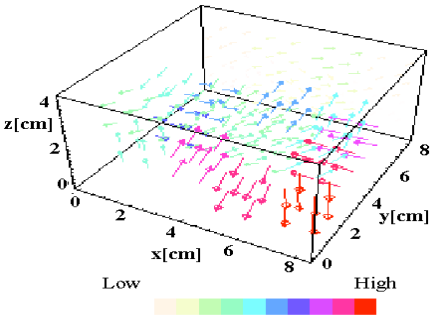

(b) Level p=2

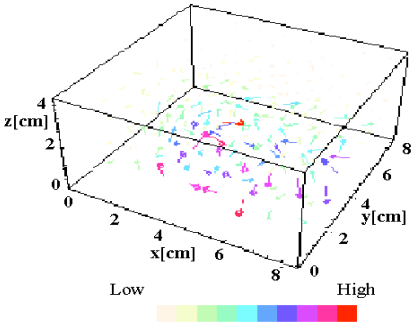

(c) Level p=3

Fig.8 Wavelets multi-resolution analysis results of the magnetic field vector distribution measured around the transformer employing U shape cores.

This means that the levels 2 and 3 magnetic fields vectors are spreading around cores centering the air gap. This spreading magnetic field vector distribution causes the electromagnetic compatibility problem.

3.3 Wavelets analysis of the magnetic field vector distribution around the transformer

Fig.9 shows the wavelets spectra of the magnetic field vectors distribution shown in Fig.6, where Daubechies second order base function is employed. The most dominant wavelets spectrum vectors are extracted as observed in Fig. 9.

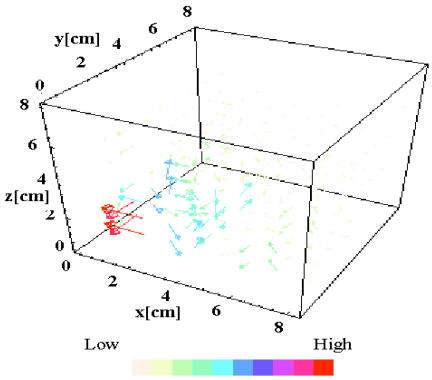

Fig.9 Wavelets spectra of the magnetic field vector distribution measured around the flat transformer.

Because of just the same reason as described in section 3.2, number of data in z-axis and also employed Daubechies second order base function, it is possible to obtain the three levels multi-resolution magnetic field vector distributions.

Fig. 10 shows the magnetic field vector distributions in each level.

The results of the wavelets multi-resolution analysis to the flat transformer suggest that major magnetic fluxes linking both of the primary and secondary cores are the levels 1 and 2 magnetic field vectors. Even though the

Copyright © 2013 Hosei University

level 3 magnetic field vectors starts from primary core and return to the same primary core, it is possible to reveal that they are regularly distributing along with the surface of primal core as well as coil.

This means that the flat transformer minimizes the leakage magnetic fields from the air gap space between the primary and secondary core surfaces.

Thus, the flat transformer has far excellent magnetic field vector distribution characteristic from the viewpoint of the electromagnetic compatibility.

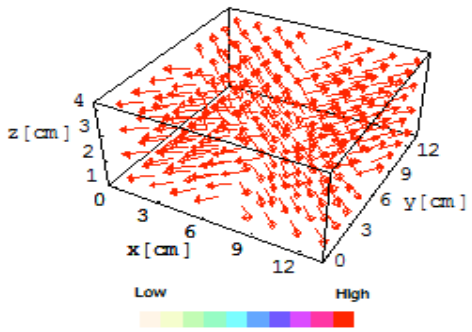

(a) Level p=1

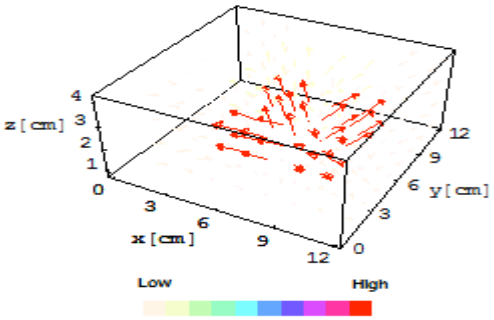

(b) Level p=2

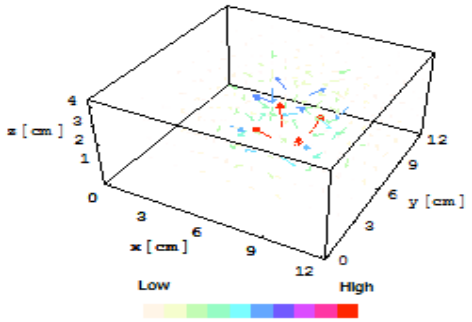

(c) Level p=3

Fig.10 Wavelets multi-resolution analysis results of the magnetic field vector distribution measured around air-gap of the flat transformer.

4 Fundamental Characteristics of the Flat Transformer

4.1 Coupling factor

A coupling factor κ is one of the most important transformer characteristics , which indicates smallness of the leakage magnetic field vectors between the primary and secondary coils. Namely, as possible as large coupling factor κ means as possible as small magnetic field vector distribution around the transformer.

Copyright © 2013 Hosei University

Let us consider a simplified circuit model of the transformer shown in Fig. 11 to evaluate the coupling factor κ. The dots '·' shown over the primary and secondary coils in Fig. 11 show the positive induced voltages at each of the coil terminals.

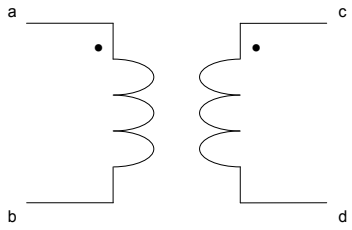

Fig.11 Simplified circuit model of transformer to evaluate the coupling factor κ.

When we connect each of the terminals in Fig. 11 to additive polarity as shown in Fig. 12(a), it is possible to obtain the following relationship:

$$L_a = L_1 + L_2 + 2M\,, \tag{6}$$

where L_a, L_1, L_2 and M are the additive-, primary self-, secondary self- and mutual inductance, respectively.

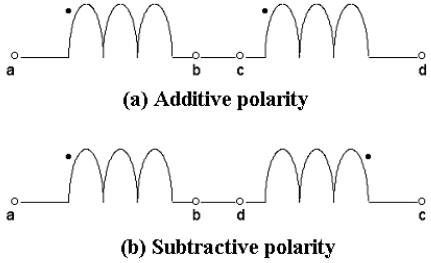

Fig.12 Series connection of the primary and secondary coils shown in Fig. 11.

Also, when we connects each of the terminals in Fig. 11 to subtractive polarity as shown in Fig. 12(b), we have

$$L_s = L_1 + L_2 - 2M\,, \tag{7}$$

where Ls is a subtractive-inductance.

Further, the primary and secondary self inductances can be measured independently. Thereby, combination of (6) and (7) leads to the mutual inductance M and coupling factor, which are respectively given by the following equations

$$M = \frac{L_a - L_s}{4}, \qquad k = \frac{M}{\sqrt{L_1 L_2}}. \tag{8}$$

Table 3 shows the measured inductances L_a, L_s, L_1, L_2 and coupling factor κ changing the air-gap length between the primary and secondary core surfaces.

Table 3 Coupling factor of the transformer employing flat shape cores measured at 30kHz.

Gap[mm]	0	1	3	5	7	10
L_1[μH]	578.6	348.2	231.1	181.6	169.9	133.9
L_2[μH]	572.7	348.1	229.4	181.0	168.3	133.3
L_s[μH]	2297.4	1358.2	881.8	669.4	617.6	450.8
L_o[μH]	16.9	26.1	41.4	56.0	61.1	84.3
κ	0.99	0.96	0.91	0.84	0.82	0.69

Copyright © 2013 Hosei University

The results listed in Table 3 suggests that the flat transformer is capable of keeping the good coupling factors $\kappa \approx 0.7$ although the primary and secondary coils are separated by air-gap of 1cm.

4.2 Power transmission rate

Power transmission rate is the other important characteristic, which indicates the efficiency of the transformer.

To improve the transformer efficiency, a secondary resonance between the capacitor and secondary leakage inductance is widely used and well known technique [4].

Fig. 13 shows a simplified circuit model attaching a resonant capacitor C.

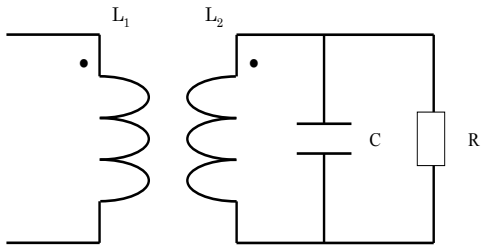

Fig. 13 Circuit diagram of a secondary resonant type transformer.

Attaching 40μF resonant capacitor in parallel to the secondary coil terminal of the flat transformer leads to a nearly $\varepsilon \approx 80\%$ input power transmission rate defined by

$$\varepsilon = \frac{\text{Secondary output power}}{\text{Primary input power}} \times 100[\%]. \qquad (9)$$

4.2 Multi-resolution analysis of the flat transformer under load condition

As described in Section 3.2, we have described about the magnetic field vector distribution and its wavelets multi-resolution analysis results. To demonstrate the usefulness of the flat transformer, it must be demonstrated that the transformer under loaded condition never stimulate the magnetic field vectors around the transformer centered at air gap.

Fig. 14 shows a measured magnetic field vector distribution at some instance of the flat transformer under the 1Ω pure resistive load and secondary resonant conditions. Measurement conditions and method of the magnetic field vectors is just the same as that of Section 2.2.

Observe the magnetic field vector distribution in Fig. 14 reveals that the flat transformer under the loaded condition reduces the entire magnetic field vectors due to the secondary load current.

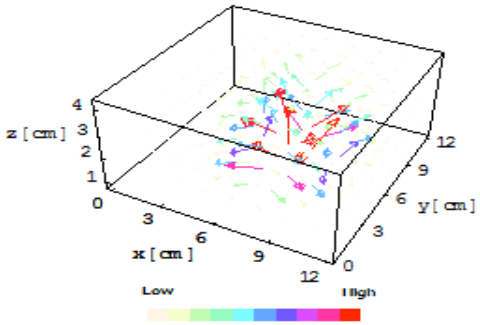

Fig.14 Magnetic field vector distribution of the flat transformer under the 1Ω pure resistive load and secondary resonant conditions.

Further, a discrete wavelets multi-resolution analysis to this magnetic field vector distribution shown in Fig. 15 reveals that the magnetic field vectors at level p=3 focus on the center of spirally wound primary coil. This means that the leakage magnetic flux is dramatically reduced compared with those of under no load condition shown in Fig. 10(c).

Copyright © 2013 Hosei University

Also, comparison the wavelets multi-resolution results shown in Fig. 11 with that of Fig. 15 suggests that the level p=2 as well as level p=3 demonstrate the dramatic reducing of the magnetic field vectors spreading to the outside direction from the center of both primary and secondary coils.

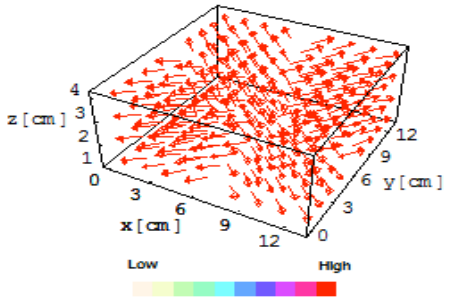

(a) Level p=1

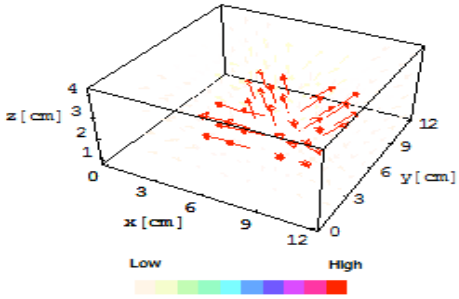

(b) Level p=2

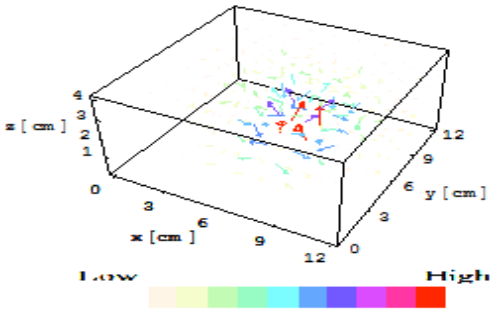

(c) Level p=3

Fig.15 Results of the wavelets multi-resolution analysis to the flat transformer under the 1Ω pure resistive load and secondary resonant conditions.

To check the secondary resonance circuit effect, we have carried out the discrete wavelets multi-resolution analysis to the magnetic field vector distribution of flat transformer under the 1Ω pure resistive load and secondary non-resonant conditions.

Fig.16 show a level p=3 magnetic field vector distribution of the wavelets multi-resolution analysis results.

One of the big differences between the level p=3 field vector distributions shown in the Figs. 15(c) and 16 is that the most dominant vectors located at the center take the opposite directions. Namely, the dominant vectors in Fig. 15(c) direct toward the center but that of Fig. 16 direct toward the outward from the center. Thus, it is clarified that the resonance of secondary circuit increases the linkage flux to the secondary coils. This leads to a highly efficient power transmission rate.

Copyright © 2013 Hosei University

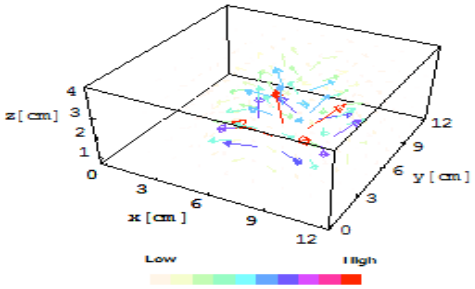

Fig.16 Level p=3 magnetic field vector distribution of the flat transformer under the 1Ω pure resistive load and secondary non resonant conditions.

5. CONCLUSIONS

To develop the contactless power suppliers, this paper has worked out one of the reasonable transformers having open magnetic flux path.

The reasons why the flat transformer is one of the most reasonable transformers are as follows.

At first, our proposed transformer suppresses the leakage magnetic fields around the core, because it is a natural extension of the shell type core structure.

Second, by means of the multi-resolution analysis of the discrete wavelets, the primary and secondary coils wound spirally focus on the magnetic field vectors to the center of both primary and secondary coils. Finally, even though the air gap is relatively large and small coupling factor, it is possible to transmit the electrical power from the primary to the secondary circuits with relatively high efficiency.

One of the drawbacks of the exploited transformer is a weight compared with those of core type transformer.

REFFE RENCES

[1] S.Takada, Y.Saito and K.Horii、Visualization of the magnetic field vectors around the contact-less power suppliers, Japan Society of Visualization, Proceedings of the Visualization Symposium in 2000, Paper No. P01-001.

[2] S.Matsuyama, S.Matsuyama, Y.Saito, Data Handling Methodology for Discrete Wavelets and Its Application to The Dynamic Vector Fields, International Journal of Wavelets, Multiresolution and Information Processing, Vol.4, No.2, June (2006) pp.263-271. World Scientific Publishing Company.

[3] S.Matsuyama, Y.Oguchi, Y.Saito, T.L.Kunii, Handling Technique of the Dynamic Color Computer Graphics by the Wavelets transform, Japan Society of Visualization, Proceedings of the Visualization Symposium in 1999, Paper No. 206.

[4] Harrison, J.L., A new resonance transformer, Electron Devices, IEEE Transactions on Issue Date: Oct 1979 Vol.26 Issue: 10, pp. 1545 - 1

Copyright © 2013 Hosei University